(Article begins on next page)

Author's Accepted Manuscript

Data fusion of electronic eye and electronic tongue signals to monitor grape ripening

G. Orlandi, R. Calvini, G. Foca, L. Pigani, G. Vasile Simone, A. Ulrici

Cite this article as: G. Orlandi, R. Calvini, G. Foca, L. Pigani, G. Vasile Simone and A. Ulrici, Data fusion of electronic eye and electronic tongue signals to monitor grape ripening, *Talanta*, https://doi.org/10.1016/j.talanta.2018.11.046

Data fusion of electronic eye and electronic tongue signals to monitor grape ripening

G. Orlandi[1], R. Calvini[1,2], G. Foca[1,2], L. Pigani[2,3], G. Vasile Simone[3], A. Ulrici[1,2*]

[1] Dipartimento di Scienze della Vita, Università di Modena e Reggio Emilia, Padiglione Besta, Via Amendola, 2 – 42122 Reggio Emilia

[2] Centro Interdipartimentale BIOGEST-SITEIA, Università degli Studi di Modena e Reggio Emilia, Piazzale Europa, 1 – 42122 Reggio Emilia

[3] Dipartimento di Scienze Chimiche e Geologiche, Università degli Studi di Modena e Reggio Emilia, Via G. Campi, 103 – 41125 Modena

*alessandro.ulrici@unimore.it

Abstract

Two separate artificial sensors, an electronic eye (EE) and an electronic tongue (ET), were recently developed to monitor grape ripening based on the analysis of must. The aim of this research is to exploit the complementary information obtained by means of EE and ET sensing systems using different data fusion strategies, in order to develop an integrated device able to quickly and easily quantify the physico-chemical parameters that are used to assess phenolic ripeness. To this purpose, both low-level and mid-level data fusion approaches were investigated. Partial Least Squares (PLS) regression was applied to the fused data, with the aim of relating the information brought by the two sensors with twelve physico-chemical parameters measured on the must samples by standard analytical methods. The results achieved with mid-level data fusion outperformed those obtained using EE and ET separately, and highlighted that both the artificial sensors have made a significant contribution to the prediction of each one of the considered physico-chemical parameters.

Graphical Abstract:
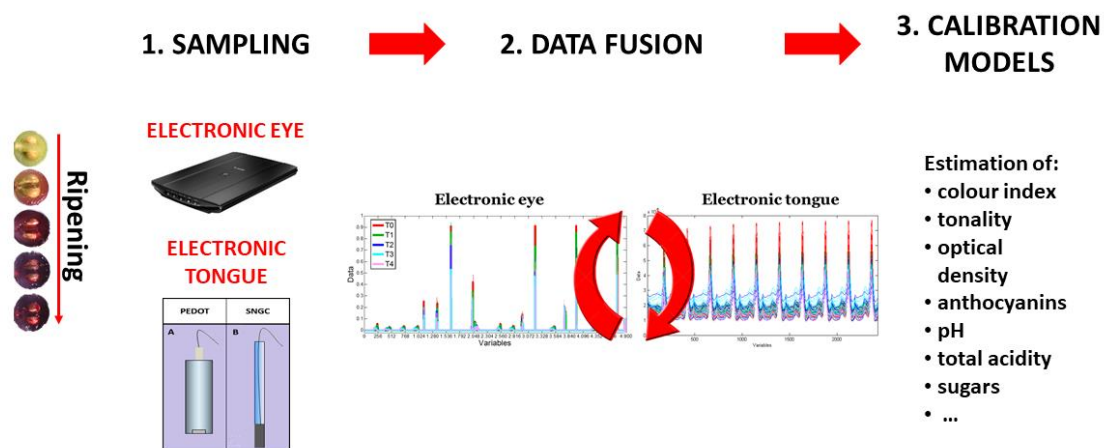
1. Introduction

The growing interest towards quality attributes of food products by consumers and producers implies the development of increasingly efficient analytical systems to monitor the quality of the final product [1]. In this context, the use of artificial sensing systems allowing to minimise sample manipulation, such as electronic noses (EN) [2,3], electronic tongues (ET) [4,5] and electronic eyes (EE) [6,7], can be an advantageous solution in order to determine specific analytes or to estimate the overall quality given by "smell", "taste" and "colour" of the analysed sample. Basically, EN and ET are non-specific sensor systems able to interact with volatile compounds and analytes dispersed in solution, respectively; for this reason, EN and ET systems are somehow related to the human senses of smell and taste. Conversely, EE is designed to analyse the colour- and aspect-related attributes of a sample that are detected by the human eye, and it is usually based on computer vision, colourimetry or spectrophotometry [8-12].

In the same way as the human brain combines the information resulting from multiple senses in order to gain a more accurate knowledge about a given object, the combination of datasets resulting from different artificial sensors can provide comprehensive information about the sample, which could not be acquired by analysing the block of data separately from each other [13,14]. Therefore, data fusion techniques are nowadays frequently used in chemometrics and several examples about the combination of different analytical techniques are reported in the literature [15-18]. In the field of artificial sensors, the use of combined ET and EN sensing systems has been frequently adopted

[19-24], whereas the use of combined systems including an EE sensing system is less common [11,12,25].

Data fusion methodologies are categorised in different ways, according to the field of application in which they are involved [26]. In chemometrics, three main levels are generally used to describe data fusion strategies [27]:

- low-level data fusion, which consists in joining directly the data from different sources;
- mid-level data fusion, which is an approach oriented to the fusion of features selected or extracted from each separate dataset by means of proper data analysis techniques;
- high-level data fusion, in which each block of data is independently analysed and the outputs of the different models are then combined to produce a final response.

In this work, our interest was focused on the evaluation of grape ripening, which is an important factor playing a fundamental role in determining the quality of the resulting wine [28]. The measurement of the different parameters defining technological and phenolic maturity of grapes requires the use of several analytical techniques, including titrimetry, refractometry, pH measurements, UV-Vis spectrophotometry, high-performance liquid chromatography (HPLC) and sensory analysis [29-33]. On the one hand, these classical analytical techniques and human taste panels represent very accurate methods for the evaluation of the parameters related to the maturity level of grapes. On the other hand, some of these techniques have inherent limitations due to their costs, the long times needed to perform the analyses and even the operator's experience. These drawbacks are particularly evident for HPLC analyses, which require skilled personnel and are quite expensive and time-consuming. The same applies to sensory analysis, which is generally time-consuming, needs a high number of trained assessors, and is prone to assessors subjectivity [34].

In two recently published papers, some of us have demonstrated the possibility of using alternative methods, such as EE [8] and ET [35], to evaluate the main parameters which are commonly used to estimate technological and phenolic maturity of grapes. The use of EE and ET has been tested on must samples derived from purple grape berries collected in the period ranging from veraison to maturity.

Briefly, the procedure involving the use of the EE sensing system was based on the following main steps: aliquots of must were dropped on absorbent paper sheets, which were then imaged using a flatbed scanner. The RGB images of the must spots were then converted into *colourgrams*, which are signals codifying the image colour properties useful for the quantification of the parameters related to the phenolic maturity of the samples.

The ET sensing system consisted of two voltammetric sensors, namely a poly-ethylendioxythiophene modified Pt electrode and a Sonogel-Carbon electrode, which were used to

3

estimate the parameters related to technological and phenolic maturity of the grape samples. The electrochemical signals were acquired directly in the must by differential pulse voltammetry, without the need of any additional reagent.

For each block of signals (EE and ET), calibration models were developed using Partial Least Squares (PLS) and the variable selection algorithm interval-Partial Least Squares (iPLS), with the aim of defining the correlation between the signals derived from the must samples and a series of physico-chemical parameters related to grape ripening, determined by reference analytical methods. In the present work, which constitutes a follow up of these former investigations, we propose the combination of EE and ET sensing systems using different data fusion strategies, in order to enhance the prediction of twelve parameters related to grape phenolic maturity. The combination of the signals obtained by EE and ET was carried out considering both low-level and mid-level data fusion strategies. In particular, to perform mid-level data fusion, two approaches were followed considering, in the first case, the variables selected and, in the second case, the latent variables (LVs) extracted from the iPLS models calculated on each separate sensor for each chemical parameter of interest. Afterwards, calibration models were built on fused datasets by means of PLS considering different data preprocessing methods and, finally, the results obtained from data fusion approaches were compared with those obtained using the separate sensors.

Material and methods

1.1 Sample collection and chemical analysis

The experiments were performed considering three different Italian purple grape varieties, namely *Ancellotta* (A), *Lambrusco Marani* (L) and *Malbo Gentile* (M). The grape samples were harvested during vintage 2015 in an experimental vineyard located in Reggio Emilia (Italy). For each variety, grape samples were collected from three grapevines (field replicates) at 5 time intervals of about 10 days (T0, T1, T2, T3, T4) from veraison to complete maturation. The 45 collected samples (= 3 field replicates $\times$ 5 time intervals $\times$ 3 grape varieties) were kept at refrigerated temperature during transportation to the laboratory, where they were immediately squeezed into a falcon tube under N_2 atmosphere to avoid the oxidation of phenolic compounds. The squeezed berries were macerated for one hour at 4°C in dark conditions and then the macerate was centrifuged at 4000 rpm for 15 minutes. The supernatant, from here onwards referred to as "must", was subdivided in two aliquots to obtain different replicates for each sample and then stored at -20°C. The must aliquots were unfrozen just before electrochemical analysis and image acquisition, that were performed in parallel with spectrophotometric and chromatographic analyses.

4

The must samples were analysed twice during two subsequent acquisition sessions, each time following a different random order. Thus, 90 analyses were carried out on the whole (= 45 samples $\times$ 2 analytical replicates).

Table 1 summarizes the twelve chemical parameters determined on the must samples to estimate the grape phenolic maturity. Additional details about the analytical procedures adopted to obtain the chemical parameters are given in Orlandi et al. [8] and Pigani et al. [35].

2.2 Electronic Eye

The key steps followed for the sample analysis by means of EE are illustrated in the left side of Figure 1.

RGB images were acquired on white paper sheets spotted with the must samples. Two different must samples were deposited on each A4-size sheet following a 4×4 chessboard scheme, where amounts of 50 µl of each must were deposited in alternate slots to finally give 8 spots per sample. The images of each paper sheet were then captured with a flatbed scanner (CanoScan Lide 220).

Firstly, an image standardisation based on standard colour references included in the image scene was performed to reduce possible discrepancies due to instrumental instability. For a more detailed description about image acquisition and the algorithms employed to standardise the images, the reader is referred to Orlandi et al. [8].

Then, the image area of each spot of must was cropped and saved as a separate image with constant pixel size (900 × 900 pixels). In our previous work, the images of the eight spots belonging to the same must sample were considered as separate items, with the purpose of estimating the within-sample variability of the EE-based approach. Instead, in the present work, in order to match the samples of EE and ET datasets, the images of the eight spots of the same must sample were concatenated into a single image with size equal to 1800 × 3600 pixels, obtaining a dataset including 90 concatenated images.

Prior to colourgrams calculation, the background pixels corresponding to the white paper sheet were removed from each concatenated image, following the same procedure described in Orlandi et al. [8]. Briefly, the analysis of the frequency distribution curves of relative red (rR, defined as the ratio between the R channel and the sum of R, G and B) highlighted that the rR values of the background (white) pixels where always lower than 0.34, conversely to the rR values of the must spot pixels; thus, background pixels were removed based on this threshold value.

For the creation of the corresponding colourgram, each image is unfolded in a two-dimensional matrix with as many rows as the number of pixels retained after background removal and three columns corresponding to the R, G, and B channels. Further colour-related parameters are then

5

calculated directly for each pixel from the R, G and B values, as described in detail in Antonelli et al. [42]: lightness (L = R + G + B), relative colours (rR = R / L, rG = G / L; rB = B / L), the hue, saturation and intensity values of the corresponding HSI colour space, and the PCA score vectors calculated on the RGB matrix considering raw, meancentered and autoscaled data (9 score vectors, i.e. 3 for each one of the 3 PCA models). Based on the results obtained in previous applications of this approach, this set of parameters is adequate to describe in detail the colour features of the analysed images. Then, for each one of the 19 colour-related parameters, the corresponding 256-points-long frequency distribution curves are calculated, merged in sequence and normalized by dividing each value by the number of pixels retained after background removal. Finally, the eigenvalues and the loading vectors of the 3 PCA models are merged at the end of the signal. The resulting signal, containing 4900 variables, is the colourgram.

The software used to standardize the images (*RGB Image Correction GUI*) and to convert them into colourgrams (*Colourgrams GUI*) has been developed in the MATLAB environment (ver. 9.2, The Mathworks Inc., USA) by some of the authors of the present work, and is freely available upon request at www.chimslab.unimore.it.

2.3 Electronic Tongue

The measurements were carried out by an Autolab PGSTAT 12 electrochemical instrument (Ecochemie) equipped with the data acquisition software GPES, using a single compartment three-electrode cell at room temperature and under Ar atmosphere. A glassy carbon rod (Methrom) and an Ag/AgCl electrode (Metrohm) served as counter and reference electrodes, respectively. All the potential values given are referred to this reference electrode.

Two voltammetric sensors were used: a Pt electrode coated by a poly-ethylendioxythiophene film (PEDOT-electrode), prepared following the procedure described in Pigani et al. [35], and a Sonogel-Carbon electrode (SNGC-electrode), prepared as described in Cubillana-Aguilera et al. [43].

The voltammetric signals were measured in the must samples without any sample pretreatment by Differential Pulse Voltammetry (DPV). Ten subsequent DPV scans were performed in the potential range − 0.30 ÷ + 0.70 V and − 0.10 ÷ + 1.00 V for the PEDOT-electrode and for the SNGC-electrode, respectively. For each one of the two electrodes, the signal that was used for the subsequent data fusion step was obtained by joining in sequence the ten subsequent scans. As it was already highlighted in previous works [35,44], this signal can be considered as a fingerprint of the corresponding sample, where both the shape of the single scans and the changes observed among different scans could bring information useful for calibration of the parameters of interest.

6

The voltammetric signals obtained by PEDOT and SNGC-electrode are reported in the right side of Figure 1. The overall configuration of the system and the operating procedures have been reported more in detail in Pigani et al. [35].

2.4 Data fusion

Before the application of data fusion approaches, the datasets have been preprocessed separately from each other. In particular, as suggested by a preliminary screening and by our previous experience with similar datasets of EE and ET data, the matrix of the EE-signals, with size equal to {90 signals, 4900 colourgram variables}, was preprocessed by meancentering, while both the PEDOT-electrode data matrix with size equal to {90 signals, 2430 potential values} and the SNGC-electrode data matrix with size equal to {90 signals, 2680 potential values} were preprocessed by 1st order derivative (Savitzky–Golay algorithm, 15 window width and 2nd order polynomial) followed by meancentering.

Then, both low-level and mid-level data fusion approaches were considered; Figure 2 reports a scheme summarizing the data fusion techniques used to combine the three blocks of signals.

In low-level data fusion the different blocks of signals are simply concatenated, obtaining a unique data matrix with a number of rows equal to the number of samples, and a number of columns equal to the sum of the variables from each block. In this work, the size of the low-level data fusion matrix was equal to 90 rows (samples) and 10010 columns (= 4900 colourgram variables + 2430 potential values of PEDOT-electrode + 2680 potential values of SNGC-electrode).

Conversely, mid-level data fusion consists in merging together features derived from a preliminary data analysis performed separately on each single block of signals, which can be conducted using different multivariate statistical methods. In the case under investigation, each block of signals had been previously analysed by means of iPLS algorithm in order to develop calibration models for the prediction of the different parameters related to phenolic maturity. More in detail, for each block of signals one calibration model had been developed for each one of the 12 analytical parameters of interest. The outcomes of these calibration models have been then combined following two different mid-level data fusion strategies:

- Mid-level on selected variables (Mid-level-SV), which consisted in merging together the variables that had been previously selected applying the iPLS algorithm separately to each one of the three sets of signals, for each dependent variable Y_i (i.e., for each physico-chemical parameter). Therefore, 12 different datasets were obtained with size {90, $(p_i + q_i + r_i)$}, where p_i, q_i and r_i correspond to the variables selected for Y_i from the EE, PEDOT and SNGC signals, respectively. The overall number of selected variables and the number of

7

variables selected for each sensor are reported as supplementary material (Table S1). For a more detailed description of the selected regions, the reader is referred to [8, 35];

- Mid-level on latent variables (Mid-level-LV), which consisted in merging together the PLS score vectors extracted from the iPLS models calculated separately for the three sets of signals. Also in this case one dataset was obtained for each dependent variable Y_i, with size equal to $\{90, (k_i + j_i + w_i)\}$, where k_i, j_i and w_i correspond to the latent variables of the iPLS models for Y_i obtained from EE, PEDOT and SNGV signals, respectively.

Concerning the EE sensor, as it was previously described in Section 2.2, it has to be highlighted that in the previous work [8] the iPLS models were calculated considering the drops derived from the same must sample as separate objects, while in this case the eight drops of the same must were analysed jointly as a unique object. Therefore, for the EE the calibration models were recalculated considering the same variables selected from the previous models, but optimizing again the number of latent variables in order to avoid overfitting.

2.5 PLS Calibration models

Partial Least Squares (PLS) calibration models were calculated on the fused datasets to predict the values of the physico-chemical parameters related to grape ripening. To this aim, the fused datasets were split into a training set and a test set following the same procedure that was adopted when considering the single blocks of signals. More in detail, the 90 signals were subdivided in a training set including the 60 signals corresponding to the samples from two field replicates, and into a test set including the 30 signals measured on the samples of the remainder field replicate.

The PLS calibration models have been calculated on fused data considering both autoscaling (AS) and block-scaling (BS) as preprocessing methods. While autoscaling provides the same weight to all the variables of the dataset, block-scaling consists in scaling to unit variance each block of data (EE, PEDOT and SNGC). In this manner each one of the three blocks of data gives the same contribution to the calibration models regardless of the measurement units and of the number of variables belonging to each block, but at the same time the relative weights of the variables within each single block are unchanged.

The statistical parameters used to evaluate the performance of the PLS models were the Root Mean Square Error (RMSE) and the coefficient of determination (R^2); both the parameters were calculated in calibration (RMSEC, R^2_{Cal}), in cross-validation (RMSECV, R^2_{CV}) and in prediction of the test set (RMSEP, R^2_{Pred}). Two deletion groups were considered for cross-validation, corresponding to the two field replicates included in the training set, and the number of latent variables was selected based on the minimum RMSECV value.

In order to evaluate the efficiency of the data fusion strategies in comparison with the results achieved using separate sensors, for each Y_i parameter the corresponding Relative Performance (RP_i) value was calculated as the ratio between the RMSEP value obtained from a single sensing system (EE or ET) and the RMSEP value obtained from each data fusion method (low-level, mid-level-SV and mid-level-LV). Therefore, RP allows to verify if data fusion (DF) leads to an increase (RP > 1) or to a decrease (RP < 1) of the model performance compared to the separate sensor (SS) [45]

$$RP_i = \frac{RMSEP(SS,i)}{RMSEP(DF,i)} \qquad (1)$$

All the calibration models were calculated using the PLS Toolbox (ver 8.5, Eigenvector Research Inc., USA).

3 Results and discussion

3.2 Modelling of fused datasets

Table 2 reports the results of the best calibration models, where for each Y parameter and each data fusion approach the preprocessing method leading to the lowest RMSECV value was selected.

Generally, block-scaling allowed to obtain better model performances compared to autoscaling. As a matter of fact, block-scaling resulted to be the best data preprocessing method in the majority of the PLS models (twenty-two out of thirty-six models).

In general, satisfactory results were obtained for ten out of twelve parameters related to grape phenolic ripening, with R^2_{Pred} values ranging from 0.63 for the quantification of Df-3-glc, to 0.95 for the estimation of Ton and CI. Conversely, it was not possible to obtain a good estimate of OD620% and of Cn-3-glc. The poor prediction of OD620% is ascribable to very low S/N ratio at 620 nm, as it was already observed in Orlandi et al. [8] and Pigani et al. [35]. Regarding Cn-3-glc, analogous results were obtained also using the separate sensors, showing poor correlation between the amount of this anthocyanin in the must samples and the corresponding EE and ET signals.

Considering the different approaches used for data fusion, the low-level method, which is simply based on the concatenation of the signals, led to lower results for the prediction of all the Y parameters compared to both the mid-level strategies. More in detail, the parameters which presented a greater improvement of model performances from a low-level to a mid-level data fusion approach are: TF (from $R^2_{Pred} = 0.58$ with low-level data fusion to $R^2_{Pred} = 0.73$ with mid-level-LV data fusion), Pt-3-glc (from $R^2_{Pred} = 0.74$ with low-level data fusion to $R^2_{Pred} = 0.90$ with mid-level-LV data fusion) and Pn-3-glc (from $R^2_{Pred} = 0.53$ with low-level data fusion to $R^2_{Pred} = 0.88$ with mid-level-LV data fusion).

Besides improving model performances, mid-level data fusion has the advantage of decreasing the number of considered variables, retaining only the relevant features (i.e., selected variables or latent variables) and disregarding all the non-informative descriptors, which implies also a reduction of the time needed for models calculation.

By comparing the results obtained using the two different mid-level data fusions strategies, the most satisfactory performances for the prediction of the Y parameters were achieved with mid-level-LV, which consisted in merging together the latent variables extracted from the iPLS models calculated on the separate sensors.

It must be highlighted that the number of variables involved in the mid-level-LV data fusion approach is further shortened with respect to mid-level-SV, since the relevant information is usually condensed in few latent variables and, therefore, it is possible to handle a small subset of variables without any leak of information. In the specific case under investigation, the higher number of latent variables involved in mid-level-LV data fusion is equal to 15 for the prediction of Df-3-glc and Mv-3-glc, which is a much smaller number of variables compared not only to the 10010 original variables considered in low-level data fusion, but also to the number of variables of the corresponding mid-level-SV models (2244 for Df-3-glc and 2024 for Mv-3-glc).

The overall best calibration models were obtained for Ton and CI ($R^2_{Pred} = 0.95$), which are useful attributes to evaluate the colour of must (and wine) samples. Equivalent results were also achieved for the quantification of TAnt ($R^2_{Pred} = 0.94$), OD420% ($R^2_{Pred} = 0.94$), OD520% ($R^2_{Pred} = 0.91$), Mv-3-glc ($R^2_{Pred} = 0.90$), Pt-3-glc ($R^2_{Pred} = 0.90$) and Pn-3-glc ($R^2_{Pred} = 0.88$).

In the case of mid-level-LV data fusion, the contribution of each block of signals (EE, PEDOT, SNGC) to the prediction of each Y parameter can be evaluated using the Variable Importance in Projection (VIP) plots reported in Figure 3. As a general rule, variables with VIP scores greater than one are assumed to furnish a substantial contribution to a given model; conversely, variables with VIP scores lower than one are less important for the model [46].

In general, for the prediction of all the parameters related to grape phenolic ripening, the LV1 scores of each block of data showed VIP score values always greater than one, suggesting that both EE and ET bring relevant information, although with a different contribution. In particular, for the prediction of TF, CI, Pt-3-glc and Pn-3-glc the LV1 scores extracted from the EE data show the higher VIP score values, and thus the greater influence on the calibration models.

Regarding the two electrodes employed in the ET sensing system, the PEDOT-electrode generally showed a major contribution to the prediction of all the Y variables compared to the SNGC-electrode. The LV1 scores extracted from PEDOT signals resulted to have higher influence in the

quantification of Df-3-glc, Cn-3-glc, Mv-3-glc and Ton. EE and PEDOT-electrode contributed almost equally to the prediction of TAnt, OD420%, OD520% and OD620%.

These results confirmed that the three different sensors are complementary to each other for predicting the properties of the must samples. Indeed, each block of signals bears different pieces of information about the investigated parameters and the fusion of these data resulted to be useful for a further improvement in the evaluation of grape phenolic ripening.

3.3 Performance comparison between data fusion approaches and separate sensors modelling

To evaluate the performance improvements brought by the data fusion approaches with respect to the models built with the separate sensing systems (EE and ET), the RP values have been calculated for each Y parameter. The results are shown in Figure 4, where the RP values are reported as a heat map: a reddish colour is related to a decrease of data fusion model performances compared to the model built with the single sensing system, while a greenish colour is related to an increase of data fusion model performances.

For most of the Y parameters the prediction performances of ET were enhanced using both low-level and mid-level data fusion. In particular, significant improvements were achieved for ten out of twelve parameters by means of mid-level-LV approach. For the remainder parameters, OD620% and Cn-3-glc, the RP is equal to 1.0 and 1.06, respectively; therefore, the scarce performance for the prediction of these two parameters was not improved by using data fusion, as it has already been highlighted in the previous Section. On the other hand, the error in prediction of the parameters related to the colour properties of the must samples was halved; in fact, for these parameters the RP values resulted equal to 2.13 for TAnt, 1.96 for Ton, 2.24 for CI and 2.05 for OD420%. Therefore, the information brought by EE, which is mainly related to the colour properties of the samples, considerably improved the performance of ET for the prediction of parameters related to the phenolic ripening of grapes.

Regarding EE, significant improvements of the predictive capability were generally obtained only with mid-level-LV data fusion, while for the other data fusion methods the model performances were usually similar or slightly worse than those obtained when using only the EE data. As for the prediction of the single anthocyanins, the models that gained benefits from data fusion are those related to Pn-3-glc (RP = 1.90), Mv-3-glc (RP = 1.23) and Pt-3-glc (RP = 1.19). Interestingly, the performance of the models related to the estimation of some colour properties of the samples were also enhanced, in the case of OD520% (RP = 1.42), OD420% (RP = 1.21) and Ton (RP = 1.32). Conversely, the TAnt parameter showed a value of RP equal to 0.86, which corresponds to an increase of the prediction error when using mid-level-LV data fusion.

In general, these results confirmed that, for most of the considered parameters, the use of proper data fusion techniques to combine EE with ET can increase the predictive performance with respect to the EE sensing system alone.

Conclusions

In the present paper, the use of different data fusion strategies was investigated to condense the information brought by EE and ET sensing systems for the evaluation of grape ripening.

As a matter of fact, the two sensing systems bring complementary information pieces about the maturity of grape samples. While ET is sensitive to the concentration of the electroactive compounds of grape must, EE describes the colour features of the must samples, which in turn are related to the concentration of the coloured chemical species. Thus, thanks to the synergy of the ET and EE responses, the application of data fusion techniques allowed to consider the information brought by both the systems, improving the calibration models for the determination of a significant number of parameters related to grape phenolic ripening.

Bearing in mind that ET is also able to predict the parameters related to the technological ripeness, i.e., sugar content and total acidity, as demonstrated in [35], this work actually shows the possibility to develop a combined device based on the two different artificial sensors. In fact, although the results reported in the present paper are based on data measured using laboratory equipment, the ET and EE sensing systems could be properly modified in order to integrate them in a unique device, including e.g. disposable graphite and PEDOT electrodes printed on absorbent paper, on which a drop of must sample can be deposited. In this manner it could be possible to acquire and elaborate both the RGB image and the electrochemical signals of the must sample at the same time, and to quantify simultaneously all the parameters of interest. Such a device could constitute a fast, inexpensive and eco-friendly solution for the estimate of technological and phenolic maturity levels of grapes directly on filed, also by non-skilled personnel.

Conflict of interest

The authors declare that they have no conflict of interest.

Acknowledgements

References

[1]   E. Borràs, J. Ferré, R. Boqué, M. Mestres, L. Aceña, Data fusion methodologies for food and beverage authentication and quality assessment - A review, Anal. Chim. Acta, 891 (2015) 1-14.

[2]   A. Loutfi, S. Coradeschi, G.K. Mani, P. Shankar, J.B.B. Rayappan, Electronic noses for food quality: A review, J. Food Eng., 144 (2015) 103-111.

[3]   J. Gutiérrez, M.C. Horrillo, Advances in artificial olfaction: Sensors and applications, Talanta, 124 (2014) 95-105.

[4]   Y. Tahara, K. Toko, Electronic tongues-a review, IEEE Sens J., 13 (8) (2013) 6516019, 3001-3011.

[5]   L. Escuder-Gilabert, M. Peris, Review: Highlights in recent applications of electronic tongues in food analysis, Anal. Chim. Acta, 665 (1) (2010) 15-25.

[6]   D. Wu, D.W. Sun, Colour measurements by computer vision for food quality control - A review, Trends Food Sci. Tech., 29 (1) (2013) 5-20.

[7]   P. Jackman, D.W. Sun, Recent advances in image processing using image texture features for food quality assessment, Trends Food Sci Technol., 29 (1) (2013) 35-43.

[8]   G. Orlandi, R. Calvini, L. Pigani, G. Foca, G. Vasile Simone, A. Antonelli, A. Ulrici, Electronic eye for the prediction of parameters related to grape ripening, Talanta, 186, (2018) 381-388.

[9]   G. Orlandi, R. Calvini, G. Foca, A. Ulrici, Automated quantification of defective maize kernels by means of Multivariate Image Analysis, Food Control, 85 (2018) 259-268.

[10]   G. Foca, F. Masino, A. Antonelli, A. Ulrici, Prediction of compositional and sensory characteristics using RGB digital images and multivariate calibration techniques, Anal. Chim. Acta, 706 (2) (2011) 238– 245.

[11]   C. Apetrei, I.M. Apetrei, S. Villanueva, J.A. de Saja, F. Gutierrez-Rosales, M.L. Rodriguez-Mendez, Combination of an e-nose, an e-tongue and an e-eye for the characterisation of olive oils with different degree of bitterness, Anal. Chim. Acta, 663 (1) (2010) 91-97.

[12]   S. Buratti, C. Malegori, S. Benedetti, P. Oliveri, G. Giovanelli, E-nose, e-tongue and e-eye for edible olive oil characterization and shelf life assessment: A powerful data fusion approach, Talanta, 182 (2018) 131-141.

[13]   A.R. Di Rosa, F. Leone, F. Cheli, V. Chiofalo, Fusion of electronic nose, electronic tongue and computer vision for animal source food authentication and quality assessment - A review, J. Food Eng., 210 (2017) 62-75.

[14]   S. Kiani, M. Saeid, M. Ghasemi-Varnamkhasti, Fusion of artificial senses as a robust approach to food quality assessment, J. Food Eng., 171 (2016) 230-239.

[15]   M. Silvestri, A. Elia, D. Bertelli, E. Salvatore, C. Durante, M. Li Vigni, A. Marchetti, M. Cocchi, A mid level data fusion strategy for the Varietal Classification of Lambrusco PDO wines, Chemom. Intell. Lab. Syst., 137 (2014) 181-189.

[16]   M. Casale, C. Casolino, P. Oliveri, M. Forina, The potential of coupling information using three analytical techniques for identifying the geographical origin of Liguria extra virgin olive oil, Food Chem., 118 (2010) 163-170.

[17]   J. Forshed, H. Idborg, S.P. Jacobsson, Evaluation of different techniques for data fusion of LC/MS and 1H-NMR, Chemom. Intell. Lab. Syst., 85 (2007) 102-109.

[18]   R. Calvini, G. Foca, A. Ulrici, Data dimensionality reduction and data fusion for fast characterization of green coffee samples using hyperspectral sensors, Anal. Bioanal. Chem., 408 (26) (2016) 7351-7366.

[19]   M.L. Rodríguez-Méndez, J.A. De Saja, R. González-Antón, C. García-Hernández, C. Medina-Plaza, C. García-Cabezón, F. Martín-Pedrosa, Electronic noses and tongues in wine industry, Front. Bioeng. Biotechnol., 4 (2016) 81.

[20]   R. Banerjee, P. Chattopadhyay, B. Tudu, N. Bhattacharyya, R. Bandyopadhyay, Artificial flavor perception of black tea using fusion of electronic nose and tongue response: A Bayesian statistical approach, J. Food Eng., 142 (2014) 87-93.

[21]   Z. Haddi, H. Alami, N. El Bari, M. Tounsi, H. Barhoumi, A. Maaref, N. Jaffrezic-Renault, B. Bouchikhi, Electronic nose and tongue combination for improved classification of Moroccan virgin olive oil profiles, Food Res. Int., 54 (2) (2013) 1488-1498.

[22]   M. Peris, L. Escuder-Gilabert, On-line monitoring of food fermentation processes using electronic noses and electronic tongues: A review. Anal. Chim. Acta, 804 (2013) 29-36.

[23]   E.A. Baldwin, J. Bai, A. Plotto, S. Dea, Electronic noses and tongues: applications for the food and pharmaceutical industries, Sensors, 11 (2011) 4744-4766.

[24]   A. Rudnitskaya, A. Legin, Using electronic tongues and noses to assess food. CAB Reviews: Perspectives in Agriculture, Veterinary Science, Nutrition and Natural Resources, 5 (27) (2010) 1-20.

[25]   Q. Ouyang, J. Zhao, Q. Chen, Instrumental intelligent test of food sensory quality as mimic of human panel test combining multiple cross-perception sensors and data fusion, Anal. Chim. Acta, 841 (2014) 68-76.

[26]   F. Castanedo, A review of data fusion techniques, Scientific World Journal., (2013) art. no. 704504.

[27]   S. Roussel, V. Bellon-Maurel, J. Roger, P. Grenier, Fusion of aroma, FT-IR and UV sensor data based on the Bayesian inference. Application to the discrimination of white grape varieties, Chemom. Intell. Lab. Syst., 65 (2003) 209-219.

[28]   A.A. Kader, Fruit maturity, ripening, and quality relationships; Acta Hortic., 485 (1999) 203-208.

[29]   OIV, Total Acidity. (2015). Compendium of International Methods of Analysis. Available online at http://www.oiv.int/public/medias/3731/oiv-ma-as313-01.pdf.

[30]   E. Obreque-Sliera, A. Peña-Neiraa, R. López-Solísb, A. Cáceres-Mellaa, H. Toledo-Arayab, A. López-Riverab, Phenolic composition of skins from four Carmenet grape varieties (Vitis vinifera L.) during ripening, Food Sci. Technol., 54 (2) (2013) 404-413.

[31]   E. Ferrari, G. Foca, M. Vignali, L. Tassi, A. Ulrici, Adulteration of the anthocyanin content of red wines: Perspectives for authentication by Fourier Transform-Near InfraRed and 1H NMR spectroscopies, Anal. Chim. Acta, 701 (2) (2011) 139-151.

[32]   M. Le Moigne, C. Maury, D. Bertrand, F. Jourjon, Sensory and instrumental characterisation of Cabernet Franc grapes according to ripening stages and growing location, Food Qual. Pref., 19 (2) (2008) 220-231.

[33]   EU Official Gazette. L 272, Luxembourg, Oct 3, 33, 1990. Available online at http://eurlex.europa.eu/legal-content/EN/TXT/PDF/?Uri = OJ:L:1990:272:FULL&from= IT.

[34]   G. Foca, A. Ulrici, M. Corbellini, M.A. Pagani, M. Lucisano, G.C. Franchini, L. Tassi, Reproducibility of the Italian ISQ method for quality classification of bread wheats: An evaluation by expert assessors, J. Sci. Food Agric., 87 (5) (2007) 839-846.

[35]   L. Pigani, G. Vasile Simone, G. Foca, A. Ulrici, F. Masino, L. Cubillana-Aguilera, R. Calvini, R. Seeber, Prediction of parameters related to grape ripening by multivariate calibration of voltammetric signals acquired by an electronic tongue, Talanta, 178 (2018) 178-187.

[36]   R. Di Stefano, M.C. Cravero, N. Gentilini, Metodi per lo studio dei polifenoli dei vini, L'Enotecnico, XXV(5) (1989) 83-89.

[37]   R. Di Stefano, M. C. Cravero, Metodi per lo studio dei polifenoli dell'uva. Rivista di Viticoltura e di Enologia, 2 (1991) 37-45.

[38]   Y. Glories, La couleur des vins rouges. Mesure, origine et interprétation. Partie I, Connaiss. Vigne Vin, 18 (1984) 195-217.

[39]   P. Ribéreau-Gayon, Y. Glories, A. Maujean, D. Dubourdieu, Handbook of Enology Volume 2: The Chemistry of Wine Stabilization and Treatments, John Wiley & Sons. New York. 2006, p 178.

[40]   F. Chinnici, F. Sonni, N. Natali, S. Galassi, C. Riponi, Colour features and pigment composition of Italian carbonic macerated red wines, Food Chem., 113 (2) (2009) 651-657.

[41]   G. Vasile Simone, G. Montevecchi, F. Masino, V. Matrella, S.A. Imazio, A. Antonelli, C. Bignami, Ampelographic and chemical characterization of Reggio Emilia and Modena (northern Italy) grapes for two traditional seasonings: 'saba' and 'agresto', J. Sci. Food Agric., 93 (2013) 3502-3511.

[42]   A. Antonelli, M. Cocchi, P. Fava, G. Foca, G.C. Franchini, D. Manzini, A. Ulrici, Automated evaluation of food colour by means of multivariate image analysis coupled to a wavelet based classification algorithm, Anal. Chim. Acta, 515 (2004) 3-13.

[43]   L.M. Cubillana-Aguilera, J.M. Palacios-Santander, I. Naranjo-Rodríguez, J.L. Hidalgo-Hidalgo-De-Cisneros, Study of the influence of the graphite powder particle size on the structure of the Sonogel-Carbon materials, J. Sol-Gel Sci. Technol., 40 (2006) 55-64.

[44]   L. Pigani, A. Culetu, A. Ulrici, G. Foca, M. Vignali, R. Seeber, PEDOT modified electrodes in amperometric sensing for analysis of red wine samples, Food Chem., 129 (1) (2011) 226-233.

[45]   E.J. Santana, B.C. Geronimo, S.M. Mastelini, R.H. Carvalho, D.F. Barbin, E.I Ida, S.Jr Barbon, Predicting poultry meat characteristics using an enhanced multi-target regression method, Biosyst. Eng., 171 (2018) 193-204.

[46]   A. Marti, A. Ulrici, G. Foca, L. Quaglia, M.A. Pagani, Characterization of common wheat flours (Triticum aestivum L.) through multivariate analysis of conventional rheological parameters and gluten peak test indices, Food Sci. Technol., 64 (1) (2015) 95-103.

Figure 1 – Key steps followed for the elaboration of the image data (left side) and for the voltammetric signals (right side).

Figure 2 – Scheme of the data fusion approaches used to combine the EE signals, the PEDOT-electrode signals and the SNGC-electrode signals.

Figure 3 - VIP scores resulting from the mid-level-LV calibration models of each Y parameter.

Figure 4 – Heat map of the relative performance (RP) values calculated for each data fusion technique with respect to the EE (left) and ET (right) separate sensing systems.

Table 1 – List of the physico-chemical parameters determined on the must samples, along with their description, the analytical technique and the corresponding reference method.

Y parameter	Description	Method	Reference
Total flavonoids content (TF)	Derived from the absorbance value measured at 280 nm; the result is expressed as mg of (+) catechin / L.	UV-Vis spectroscopy	[36]
Total anthocyanins content (TAnt)	Derived from the absorbance measured at 540 nm; the result is expressed as mg of oenin chloride / L.	UV-Vis spectroscopy	[37]
Colour index (CI)	Sum of the absorbance values measured at 420, 520 and 620 nm.	UV-Vis spectroscopy	[38]
Tonality (Ton)	Ratio between the absorbance values measured at 420 and 520 nm.	UV-Vis spectroscopy	[39]
Optical density at 420nm (OD420%)			
Optical density at 520nm (OD520%)	Percentage contribution of each absorbance value to the colour index	UV-Vis spectroscopy	[39]
Optical density at 420nm (OD620%)			
Delphinidin 3-O-monoglucoside (Df-3-glc)			
Cyanidin 3-O-monoglucoside (Cn-3-glc)			
Petunidin 3-O-monoglucoside (Pt-3-glc)	The concentration of each anthocyanin is expressed as mg of malvidin-3-O-glucoside / L.	HPLC-DAD	[40]
Peonedin 3-O-monoglucoside (Pn-3-glc)			
Malvidin 3-O-monoglucoside (Mv-3-glc)			

16

Table 2 – Results of the best calibration models for each data fusion approach (low-level, mid-level-SV and mid-level-LV).
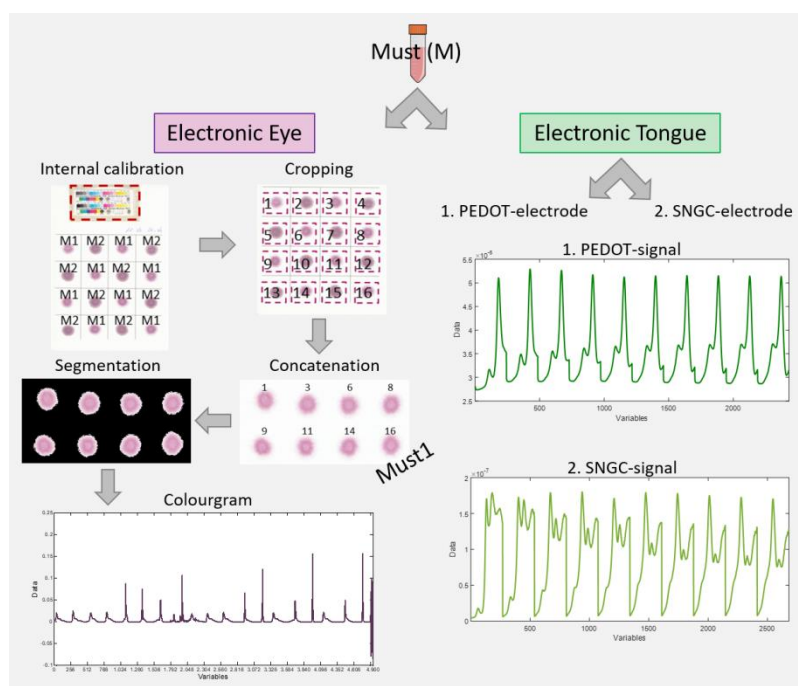
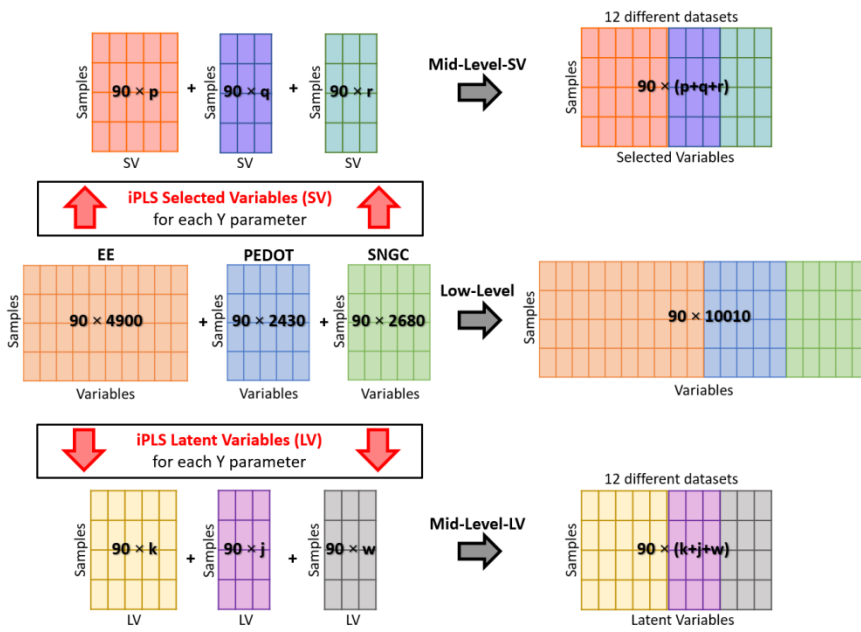| Y*	DF	Preproc.**	# Var.	LVs	RMSEC	RMSECV	RMSEP	R^2_{Cal}	R^2_{CV}	R^2_{Pred}
TF	Low-level	AS	10010	3	18,66	29,14	28,46	0,86	0,66	0,58
	Mid-level-SV	BS	1522	3	16,09	20,45	24,68	0,90	0,83	0,69
	Mid-level-LV	BS	11	3	15,28	20,43	23,13	0,91	0,83	0,73
TAnt	Low-level	AS	10010	3	19,60	31,67	26,05	0,95	0,87	0,91
	Mid-level-SV	AS	927	3	17,26	27,77	27,02	0,96	0,90	0,90
	Mid-level-LV	AS	14	5	14,62	30,13	21,85	0,97	0,88	0,94
Ton	Low-level	BS	10010	5	0,06	0,12	0,12	0,97	0,90	0,89
	Mid-level-SV	BS	1287	5	0,07	0,11	0,09	0,97	0,92	0,94
	Mid-level-LV	BS	13	5	0,07	0,09	0,08	0,97	0,96	0,95
CI	Low-level	AS	10010	3	0,90	1,43	1,00	0,93	0,82	0,92
	Mid-level-SV	AS	1866	3	0,85	1,35	1,02	0,94	0,84	0,91
	Mid-level-LV	BS	10	2	0,79	1,10	0,80	0,95	0,90	0,95
OD420%	Low-level	BS	10010	4	2,20	3,66	3,51	0,97	0,91	0,91
	Mid-level-SV	BS	735	4	2,27	2,58	3,82	0,97	0,95	0,90
	Mid-level-LV	BS	14	3	2,32	2,53	3,03	0,96	0,96	0,94
OD520%	Low-level	BS	10010	4	3,24	4,98	5,46	0,94	0,87	0,81
	Mid-level-SV	BS	1499	5	3,10	3,81	4,67	0,95	0,92	0,86
	Mid-level-LV	BS	13	5	3,19	3,60	3,76	0,95	0,93	0,91
OD620%	Low-level	BS	10010	1	1,86	2,05	1,95	0,30	0,15	-1,20
	Mid-level-SV	BS	971	1	1,81	1,97	1,96	0,33	0,21	-1,22
	Mid-level-LV	BS	5	5	1,52	1,78	1,84	0,53	0,36	-0,94
Df-3-gcl	Low-level	AS	10010	4	2,41	4,19	8,94	0,89	0,68	0,55
	Mid-level-SV	AS	2244	5	2,69	4,28	8,10	0,87	0,67	0,63
	Mid-level-LV	BS	15	4	3,33	4,31	8,68	0,80	0,66	0,58
Cn-3-gcl	Low-level	BS	10010	3	1,36	2,13	7,17	0,84	0,61	0,01
	Mid-level-SV	AS	1051	4	1,18	2,18	6,44	0,88	0,59	0,20
	Mid-level-LV	BS	14	3	1,65	1,99	6,46	0,77	0,66	0,20
Pt-3-gcl	Low-level	AS	10010	4	3,42	6,44	7,46	0,92	0,72	0,74
	Mid-level-SV	BS	1586	4	4,03	5,58	5,51	0,89	0,79	0,86
	Mid-level-LV	BS	13	3	4,03	5,07	4,64	0,89	0,83	0,90
Pn-3-gcl	Low-level	AS	10010	1	7,52	8,23	11,06	0,58	0,50	0,53
	Mid-level-SV	BS	1231	2	6,60	6,83	11,31	0,68	0,65	0,51
	Mid-level-LV	AS	11	3	3,65	4,22	5,17	0,91	0,88	0,88
Mv-3-gcl	Low-level	AS	10010	4	11,08	28,80	23,47	0,98	0,89	0,90
	Mid-level-SV	AS	2024	5	12,78	27,16	27,49	0,98	0,90	0,87
	Mid-level-LV	BS	15	4	19,68	26,97	23,60	0,95	0,90	0,90

* TF = total flavonoids content; TAnt = total anthocyanins content; Ton = tonality; CI = colour index; OD420% = optical density at 420 nm; OD520% = optical density at 520 nm; OD620% = optical density at 620 nm; Df-3-gcl = delphinidin 3-O-monoglucoside; Cn-3-gcl = cyanidin 3-O-monoglucoside; Pt-3-gcl = petunidin 3-O-monoglucoside; Pn-3-gcl = peonidin 3-O-monoglucoside; Mv-3-gcl = malvidin 3-O-monoglucoside

** AS = autoscaling; BS = block scaling.

Highlights

- Data fusion was used to improve the performance of a device to monitor grape ripening

- Data from an electronic tongue (ET) and an electronic eye (EE) were combined

- Low-level and mid-level data fusion were used to build PLS calibration models

- The use of data fusion allowed to increase significantly the prediction performances

- Mid-level data fusion of PLS latent variables gave generally the best results